

A polarization-based Thomson scattering technique for burning plasmas

This content has been downloaded from IOPscience. Please scroll down to see the full text.

2014 JINST 9 C02030

(<http://iopscience.iop.org/1748-0221/9/02/C02030>)

View [the table of contents for this issue](#), or go to the [journal homepage](#) for more

Download details:

IP Address: 128.104.165.51

This content was downloaded on 29/07/2015 at 18:57

Please note that [terms and conditions apply](#).

16th INTERNATIONAL SYMPOSIUM ON LASER-AIDED PLASMA DIAGNOSTICS,
22–26 SEPTEMBER 2013,
MADISON, WISCONSIN, U.S.A.

A polarization-based Thomson scattering technique for burning plasmas

E. Parke,¹ V.V. Mirnov and D.J. Den Hartog

*Department of Physics, University of Wisconsin-Madison,
1150 University Avenue, Madison, U.S.A.*

E-mail: eparke@wisc.edu

ABSTRACT: The traditional Thomson scattering diagnostic is based on measurement of the wavelength spectrum of scattered light, where electron temperature measurements are inferred from thermal broadening of the spectrum. At sufficiently high temperatures, especially those predicted for ITER and other burning plasmas, relativistic effects cause a change in the degree of polarization (P) of the scattered light; for fully polarized incident laser light, the scattered light becomes partially polarized. The resulting reduction of polarization is temperature dependent and has been proposed by other authors as a potential alternative to the traditional spectral decomposition technique. Following the previously developed Stokes vector approach, we analytically calculate the degree of polarization for incoherent Thomson scattering. For the first time, we obtain exact results valid for the full range of incident laser polarization states, scattering angles, and electron temperatures. While previous work focused only on linear polarization, we show that circularly polarized incident light optimizes the degree of depolarization for a wide range of temperatures relevant to burning plasmas. We discuss the feasibility of a polarization based Thomson scattering diagnostic for ITER-like plasmas with both linearly and circularly polarized light and compare to the traditional technique.

KEYWORDS: Plasma diagnostics - interferometry, spectroscopy and imaging; Analysis and statistical methods

¹Corresponding author.

Contents

1	Introduction and background	1
2	Theoretical results	2
2.1	Diagnostic implications	3
3	Diagnostic design and simulation	4
3.1	Polarization over a narrow wavelength range	6
4	Advantages and implementation challenges	9

1 Introduction and background

Standard Thomson scattering diagnostics are based on wavelength spectrum measurements of scattered light from plasmas. Thermal broadening of the laser light is used to infer electron temperature for a wide range of operating conditions from a few eV to greater than 10 keV [1, 2]. Polychromator systems with avalanche photodiodes (APDs) have become common tools for spectrally binning the scattered light and achieving high sensitivity [3, 4]. Polychromator spectral sensitivity is crucial to determining the optimal range for temperature measurements, with core and edge Thomson diagnostics relying on significantly different filter sets. For core Thomson scattering systems observing high temperature plasmas, increased thermal broadening of the scattered light as well as variable plasma conditions can necessitate the use of a large number of spectral bins or channels.

Thomson scattering diagnostics typically utilize fully polarized lasers; in addition to thermal broadening of the spectrum, the scattering process produces partially polarized scattered light. The degree of depolarization depends on the electron temperature, leading other authors to propose Thomson polarization techniques as an alternative temperature measurement diagnostic [5, 6]. The technique proposed in ref. [5] involves up to four measurements of the polarization properties of the scattered light — the Stokes vector components — and has the potential to be simpler to implement. Furthermore, if the dependence of the degree of depolarization on electron temperature is precisely known from theory, such a diagnostic could offer higher accuracy. Expected diagnostic error bars calculated in ref. [5] compared well with spectrally resolved Thomson predictions for fusion-grade temperatures.

A number of assumptions and constraints limit the results in ref. [6]. They are not universally valid for the whole range of experimental parameters such as electron temperature, scattering angle, and incident laser polarization state. These restrictions prevent a full optimization of the diagnostic scheme. Furthermore, the work in ref. [6] contains an error in the weighting factor for averaging over the electron distribution function. The results and analysis in this paper are based on an exact description of the degree of polarization presented at the IAEA Fusion Energy Conference in 2012 [7, 8]. These results are the first analytic description valid for all incident polarization states, scattering angles, and electron temperatures. The full derivation will be published elsewhere; here we present a brief outline of the approach and key theoretical results. We then apply these results to the diagnostic proposed in ref. [5].

2 Theoretical results

For the typical, wavelength resolved Thomson scattering diagnostic, the wave scattered by a single electron is calculated in the far-field zone, Fourier transformed, converted to a power spectrum, and then integrated over the electron distribution function [1, 2]. The resulting analytical power spectrum includes both thermal broadening effects, blue-shift due to relativistic electron-headlighting, and a term commonly referred to as a “depolarization factor” which includes both relativistic headlighting effects and a reduction of scattered spectral intensity due to polarization effects. In this paper we develop a more general approach which allows us to describe the conversion of fully polarized incident light to partially polarized scattered radiation. For this purpose, we follow the Stokes vector and Mueller matrix formalism of ref. [6].

We express both the scattered field, $\mathbf{S}^{(s)}$, and the incident field, $\mathbf{S}^{(i)}$, in Stokes vector form, $\mathbf{S} = (S_0, S_1, S_2, S_3)$. Here, the S_0 component corresponds to the total intensity of the wave and the remaining components describe the polarization properties. The polarization is characterized by two parameters: the ellipticity, χ , where $\chi = 0$ for linear light and $\chi = \pi/4$ for circular light, and the orientation angle, ψ , between the major axis of the polarization ellipse and the normal vector to the scattering plane ($\psi = 0$ for light aligned perpendicular to the scattering plane and $\psi = \pi/2$ for light parallel to the scattering plane). Writing the Stokes vector in terms of χ and ψ yields $\mathbf{S} = (S_0, S_0 \cos 2\chi \cos 2\psi, S_0 \cos 2\chi \sin 2\psi, S_0 \sin 2\chi)$ for completely polarized light. From the incident and scattered electric fields, we construct a 4×4 Mueller matrix describing the scattering process: $\mathbf{S}^{(s)} = \mathbf{M} \cdot \mathbf{S}^{(i)}$. We then integrate this matrix over the electron distribution function (assumed here to be an isotropic, relativistic Maxwellian). Most of the matrix elements are zero or integrate to zero. The relevant terms of the Mueller matrix are:

$$\begin{aligned}
 M_{00} &= 1 + u^2 - 2G(\mu)(u^2 + 4u - 3) + (16/\mu^2)(1 - u)^2 \\
 M_{01} &= M_{10} = 1 - u^2 \\
 M_{11} &= 1 + u^2 + 2G(\mu)(u^2 - 4u + 1) + (12/\mu^2)(1 - u)^2 \\
 M_{22} &= 2u - 4G(\mu)(u^2 - u + 1) - (12/\mu^2)(1 - u)^2 \\
 M_{33} &= 2u - 4G(\mu)u(2u - 1) - (8/\mu^2)(1 - u)^2.
 \end{aligned} \tag{2.1}$$

Where $u = \cos(\theta)$ represents the scattering angle dependence and $G(\mu) = K_1(\mu)/(\mu K_2(\mu))$ represents the temperature dependence, with $\mu = m_e c^2 / T_e$. K_1 and K_2 are modified Bessel functions of the second kind.

The work in ref. [6] contains an error in the power of the term $\kappa = (1 - \beta_s)$ originating in the Liénard-Wiechert expression for the scattered field. While there is contention in the literature over the power of this term for an infinite scattering volume, for a finite volume the appropriate term is unambiguous. At fusion-grade temperatures this can introduce non-negligible error. The results above were calculated with the correct power.

For incident light of arbitrary intensity and polarization, the scattered light can be expressed in terms of the Mueller matrix elements: for example, $S_0^{(s)} = M_{00} \cdot S_0^{(i)} + M_{01} \cdot S_1^{(i)}$. For fully polarized incident light, with $S_0^2 = S_1^2 + S_2^2 + S_3^2$, scattered light from a single electron remains completely polarized, but due to the nature of the electron distribution function, light scattered from many electrons will include photons of many different polarization states. This is described by the degree of

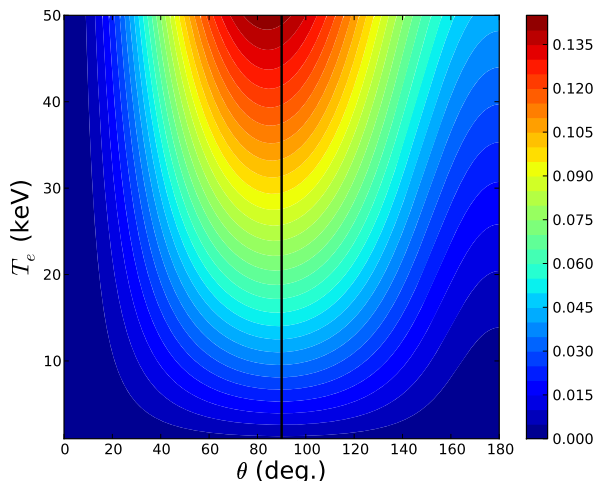


Figure 1. Degree of depolarization for linearly polarized incident light with $\psi = 0$.

polarization, $P = \sqrt{S_1^2 + S_2^2 + S_3^2}/S_0$, which can range from 0 to 1, and the degree of depolarization, $D = 1 - P$. The degree of depolarization should not be confused with the “depolarization factor” from the spectral decomposition approach mentioned above (commonly denoted by q), which denotes a reduction in scattered intensity.

2.1 Diagnostic implications

From the theoretical results above, a few constraints on diagnostic design can be determined. Both scattering angle and incident laser polarization are important parameters for Thomson scattering diagnostics. Most diagnostics operate with scattering angles near $\theta = \pi/2$ but covering a wide range, while the LIDAR Thomson system proposed for ITER would operate near $\theta = \pi$ [9]. Universal (to our knowledge) use of linearly polarized incident light with the electric field aligned perpendicular to the scattering plane originates in the simplicity offered to scattering spectrum calculation as well as optimization of scattered intensity for cold electrons.

Figure 1 shows the degree of depolarization across the full range of scattering angles and fusion relevant temperatures for linearly polarized light with $\psi = 0$. Depolarization is strongest near perpendicular scattering, although not exactly at $\theta = \pi/2$. The exact angle of maximum depolarization is temperature dependent, and these results are consistent with the findings of ref. [6] showing maximum depolarization deviating slightly from $\pi/2$. However, this is only a local maximum due to the choice of linearly polarized light — the true maximum occurs for elliptically polarized light, see figure 2(a).

Far away from $\pi/2$ scattering, the depolarization drops off rapidly. For both forward and backward scattering, the degree of depolarization is no more than a few percent for expected reactor temperatures. A polarization-based Thomson scattering technique would be highly unsuitable for diagnostics like the proposed ITER LIDAR system, while traditional Thomson scattering diagnostics near $\theta = \pi/2$ would offer greater depolarization with stronger temperature dependence.

Evaluating the effectiveness of different laser polarization parameters is slightly more complicated. Some configurations offer strong degrees of depolarization, but weak scattered intensity. In

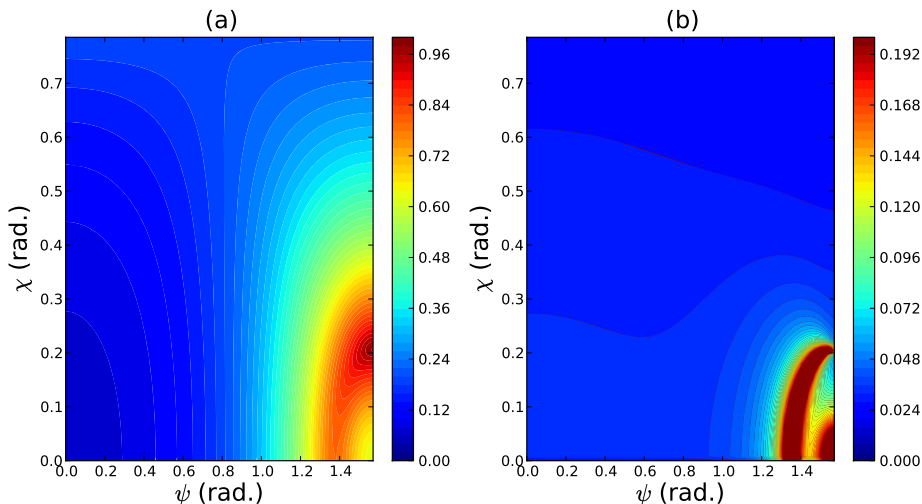


Figure 2. (a) Depolarization and (b) predicted relative error in temperature measurement for 20 keV plasmas at $\pi/2$ scattering angle with varying incident laser polarization (ellipticity χ and orientation angle ψ).

figure 2(b), the predicted relative error in the temperature measurement is plotted against both the orientation angle and the ellipticity. This includes only Poisson statistics for the scattered photons and neglects background light; background signal is accounted for in the diagnostic simulations of section 3. The region near $\psi = \pi/2$ exemplifies the high depolarization, low scattered intensity trade off: large measurement errors limit diagnostic viability and the features are highly sensitive to electron temperature, making this section of parameter space one to be avoided.

The minimum error corresponds to circular polarization. Thomson scattering literature focuses almost exclusively on linear polarization, and even ref. [6] is restricted in analysis to linearly polarized light. These results highlight the versatility of this approach and the need to consider all incident polarizations. However, it should be noted that, for the purposes of a Thomson polarization diagnostic, linearly polarized light with $\psi = 0$ can achieve error bars competitive with circularly polarized light.

3 Diagnostic design and simulation

Using the insight developed above, we further explore the viability of a polarization-based Thomson scattering diagnostic by applying our theoretical results to the proposed design in ref. [5]. The original design was intended for linearly polarized incident light with $\psi = \pi/4$, so the diagram in figure 3 has been modified slightly to enable measurements with elliptically polarized light. The four Stokes components are related to six measureable intensities, although only four of the measureable quantities are independent. For the modified diagnostic proposal, we choose three of the intensity measurements from the original design: without phase retardation, the intensity is measured after polarization selection at angles of 0° , 90° , and 135° relative to an electric field with $\psi = 0$. The fourth independent intensity measurement is obtained following phase retardation of $\pi/2$ and polarization selection at 135° (corresponding to right-hand circularly polarized light). The only modification to the original design requires removing the half-wave plate and second

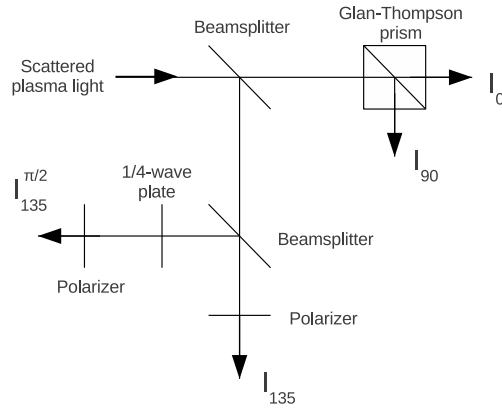


Figure 3. Polarization measurement design adapted from ref. [5], with modifications for elliptically polarized incident light.

Glan-Thompson prism, replacing them with the beamsplitter, quarter-wave plate, and appropriate polarizers in the lower right of the diagram. This would lead to a slightly more complicated mounting arrangement, but allows measurements with elliptically polarized incident light. The Stokes vectors are calculated from the measured intensities using the following relations:

$$\begin{aligned}
 S_0 &= I_{0^\circ} + I_{90^\circ} \\
 S_1 &= I_{0^\circ} - I_{90^\circ} \\
 S_2 &= I_{0^\circ} + I_{90^\circ} - 2I_{135^\circ} \\
 S_3 &= I_{0^\circ} + I_{90^\circ} - 2I_{135^\circ}^{\pi/2}.
 \end{aligned} \tag{3.1}$$

Note that $I_{\text{Stokes}} = |E|^2$ is proportional to the usual intensity definition $I_{\text{Poynting}} = \frac{1}{2}\epsilon_0 c |E|^2$.

The simulated diagnostic utilizes a laser capable of producing 5 J pulses at 1064 nm wavelength with an integration time of 10 ns. The beam waist is 20 mm and the scattering volume has length 55 mm, while the collection optics subtend a solid angle of 1.19 msr. The scattering angle is $\theta = \pi/2$ from a core location with variable electron temperature $T_e(0)$. We treat the background light as entirely bremsstrahlung, ignoring line radiation. To model the bremsstrahlung, we follow the nonrelativistic approach in ref. [1]. Relativistic effects on the bremsstrahlung spectrum are ignored as they account for less than a 10% effect at the temperatures and wavelengths used here [10]. The Gaunt factor, however, is approximated as 7. The electron temperature and density profiles are assumed to be parabolic, $T_e(r) = T_e(0) \cdot (1 - r^2)$, with core electron density of $1 \cdot 10^{20} \text{ m}^{-3}$. The background light is integrated along a 4 m line of sight and over wavelengths in the range 200–2000 nm to accommodate the full width of the scattered spectrum. These parameters are chosen for similarity with ITER.

The simulated diagnostic error bars are calculated for core temperatures ranging from 1 keV to 50 keV. Three cases are compared: $\chi = \pi/4$, $(\psi, \chi) = (0, 0)$, and $(\psi, \chi) = (\pi/6, 0)$. The circularly polarized light utilizes the full, 4-component polarimeter shown, while the linear cases utilize reduced forms: measurement of only I_{0° , I_{90° , and I_{135° for the $(\psi, \chi) = (\pi/6, 0)$ case and further reduction to only I_{0° and I_{90° for the $(\psi, \chi) = (0, 0)$ case. The reduced forms of the polarimeter benefit from improved scattered signal amplitude on the measured channels.

The polarization measurement error, σ_P , is related to the error on each of the statistically independent intensity measurements, σ_{I_j} , in the standard manner:

$$\sigma_P^2 = \sum_j \left(\frac{\partial P}{\partial I_j} \right)^2 \sigma_{I_j}^2 \quad (3.2)$$

and the intensity measurement errors are determined by Poisson statistics on both the scattered laser signal and background bremsstrahlung. The $\partial P/\partial I_j$ terms evaluate to

$$\begin{aligned} \frac{\partial P}{\partial I_{0^\circ}} &= \frac{1}{S_0} \left(-P + \frac{S_1 + S_2 + S_3}{PS_0} \right) \\ \frac{\partial P}{\partial I_{90^\circ}} &= \frac{1}{S_0} \left(-P + \frac{-S_1 + S_2 + S_3}{PS_0} \right) \\ \frac{\partial P}{\partial I_{135^\circ}} &= -\frac{2S_2}{PS_0^2} \\ \frac{\partial P}{\partial I_{135^\circ}^{\pi/2}} &= -\frac{2S_3}{PS_0^2}. \end{aligned} \quad (3.3)$$

From the error in the polarization measurement, the relative error in the temperature measurement is

$$\frac{\sigma_{T_e}}{T_e} = \frac{\sigma_P}{\mu} \frac{\partial P}{\partial \mu}. \quad (3.4)$$

The term $\partial P/\partial \mu$ is calculated numerically, as the analytical form is excessively complicated for arbitrary incident laser polarization.

The results are shown in figure 4. Above 9 keV, all cases achieve error bars of less than 5%, and less than 2% above 23 keV, making them competitive with standard Thomson scattering diagnostics. The circular polarization case offers the best performance for the full, 4-component polarimeter, and even outperforms the reduced 3-component variation. However, the 2-component polarimeter achieves the best results across the full range of temperatures, with error bars below 1% at 50 keV. The flatness of the curves above 20 keV indicates that these diagnostics would be robust over a wide range of fusion-relevant temperatures.

3.1 Polarization over a narrow wavelength range

While the scattered spectra are very broad for fusion-grade plasmas, the results in section 2 require integration over all wavelengths. As indicated by the integration of background bremsstrahlung from 200 to 2000 nm in the estimate above, the need to measure the total scattered power leads to several technical challenges. A significant fraction of the bremsstrahlung background is radiated at shorter wavelengths, and such a wide window will also include substantial contributions from line radiation (especially H_α). For silicon APDs commonly used in TS polychromator systems, the response is typically low below 400 nm and above 1100 nm, cutting off the red-shifted portion of the spectrum. Additionally, most optical components do not have uniform response over such a wide range. Frequency-doubled Nd:YAG lasers at 532 nm would produce narrower scattered spectra, but extending deeper into the UV where bremsstrahlung contributions are larger and APD responsivity is low. Choosing a laser with longer wavelength would broaden the spectrum further.

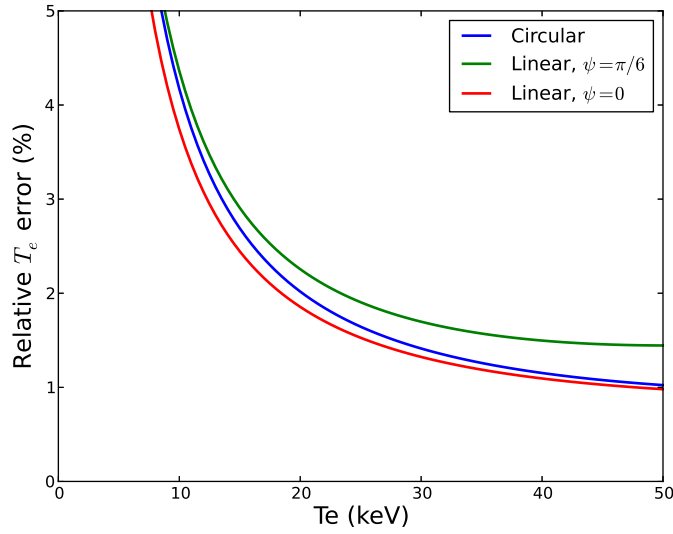


Figure 4. Predicted error in temperature measurement for three implementations of the polarization diagnostic: circular, linear with $\psi = \pi/6$, and linear with $\psi = 0$.

Realistic experimental constraints require accepting only scattered photons within a limited wavelength range. To evaluate the feasibility of a polarimeter under these conditions, we return to spectral analysis. We restrict the analysis to the case of linear incident laser light with $\psi = 0$, where only the signals I_{0° and I_{90° need to be evaluated. Following the approach in ref. [5], we integrate the scattered spectrum for two cases. From ref. [1], the scattered power is given by

$$\frac{dP}{d\omega_s} = n_e r_e^2 \langle S_i \rangle V d\Omega \int |\Pi \cdot \hat{e}|^2 f(\beta) \delta[c(\mathbf{k}_s - \mathbf{k}_i) \cdot \beta - (\omega_s - \omega_i)] d^3\beta \quad (3.5)$$

where $\Pi \cdot \hat{e}$ is a polarization tensor on the incident field, $\langle S_i \rangle$ is the incident power (Poynting), and $f(\beta)$ is the electron distribution function. The incident and scattered waves are characterized by wavenumbers \mathbf{k}_i and \mathbf{k}_s and angular frequencies ω_i and ω_s . For clarity, we reserve P for degree of polarization while $dP/d\omega_s$ or $dP/d\lambda_s$ denote the power spectrum. For linearly polarized laser light (with $\psi = 0$) and scattered light selected with polarization parallel to the incident light, this spectrum has been well studied in the literature. We use the (1,1) approximation published by Naito, et al. [11]:

$$\begin{aligned} \left(\frac{dP}{d\lambda_s} \right)_{\parallel} &= S_\omega \cdot q_{\parallel} \\ S_\omega &= \frac{n_e r_e^2 \langle S_i \rangle V d\Omega x^4}{2\lambda_i K_2(\mu) \sqrt{1+x^2-2x\cos\theta}} \exp\left(-\mu \sqrt{\frac{1+x^2-2x\cos\theta}{2x(1-\cos\theta)}}\right) \\ q_{\parallel} &= 1 - 4\eta\zeta \frac{2\zeta - \eta(2-3\zeta^2)}{2\zeta - \eta(2-15\zeta^2)} \end{aligned} \quad (3.6)$$

where $x = \omega_s/\omega_i$ and η and ζ are defined in ref. [11]. For scattered light with all polarization states

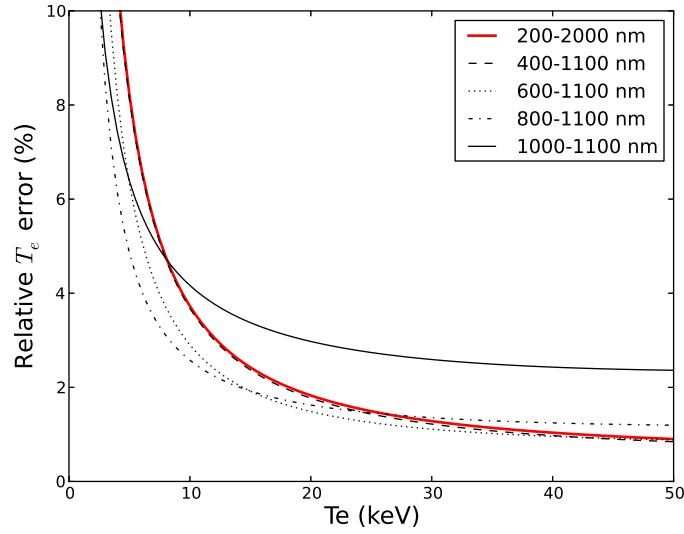


Figure 5. Predicted error in temperature measurement for different wavelength integration ranges: 200–2000 nm (red curve) to match the Stokes vector calculations, and several narrower ranges (black curves) to more accurately represent measurement conditions.

present, the form of the polarization tensor is [12]:

$$|\Pi \cdot \hat{e}|^2 = (1 - \beta^2) \frac{\omega_s^2}{\omega_i^2} \left[1 - (1 - \beta^2) \left\{ \frac{\beta_e(1 - \cos \theta)}{(1 - \beta_s)(1 - \beta_i)} \right\}^2 \right]. \quad (3.7)$$

This case is not well studied, so we also calculated the scattering spectrum in the form

$$\left(\frac{dP}{d\lambda_s} \right)_{\text{tot}} = S_\omega \cdot q_{\text{tot}} \quad (3.8)$$

where q_{tot} is obtained by numerically integrating eq. (3.5) using the form of the polarization tensor given in eq. (3.7). From this, the measured signals are $I_{0^\circ} = \left(\frac{dP}{d\lambda_s} \right)_{\parallel}$ and $I_{90^\circ} = \left(\frac{dP}{d\lambda_s} \right)_{\text{tot}} - \left(\frac{dP}{d\lambda_s} \right)_{\parallel}$, and the polarization P can be evaluated by integration of the spectra over arbitrary wavelength ranges. For sufficiently wide wavelength windows, predictions with this approach agree with the Stokes vector approach. Figure 5 shows the comparison of several different windows. Reducing the range of integration to match APD sensitivity, and further reducing the range to cut down on bremsstrahlung are beneficial for diagnostic error bars. Although the windows reject significant numbers of scattered photons, they reject a greater fraction of the background. Windows of 100 nm or less lead to higher error at high T_e , but are still below 3%. Appropriate choice of window also reduces the minimum T_e at which such a diagnostic could operate.

4 Advantages and implementation challenges

A polarization-based diagnostic offers several advantages over the polychromator design common now. With a maximum of 4 channels per radial position, the polarization diagnostic could translate into cost savings in detector hardware and digitizer channels. The need for fewer measurement channels would be less operationally demanding, while fewer optics make for a simpler, more robust diagnostic. The 2-component form of the polarimeter maximizes these advantages. The primary challenge to implementing a TS polarimeter is preserving the polarization state of the scattered light, which can be altered by both the plasma, through Faraday rotation, and the collection optics.

The estimated Faraday rotation is negligible. Overestimating the contribution with a 5 T magnetic field and a 4 m scattering path length parallel to the magnetic field, the Faraday effect rotates scattered light at 1064 nm by $5.96 \cdot 10^{-4}$ radians. Blue-shifted light will rotate less, and the actual path for both incident and scattered light will mostly be perpendicular to the magnetic field. Even at a few keV, the perpendicular polarized Thomson scattered photons will dominate the Faraday rotation contribution. Cotton-Mouton effects on scattered ellipticity are estimated to be several orders of magnitude smaller.

The collection optics pose a greater challenge. While the mirror system proposed for ITER (or the lens systems on current devices) should not significantly alter polarization, the same is not true of the fibers used to transport the collected light to detectors. Most fibers do not preserve polarization; fibers capable of preserving polarization in the wavelength range of interest are available, but expensive. Additionally, while the original design in ref. [5] makes optional use of a half-wave plate to simplify the arrangement of detectors for the I_{-45° and I_{+45° components, the full, 4-component polarization meter suggested here requires the use of a quarter-wave plate to measure the $I_{135^\circ}^{\pi/2}$ component of the scattered light. Currently available waveplates do not have a uniform response over the wide ranges of wavelengths needed, making the polarization meter unfeasible for circularly polarized light. While the 3- and 2-component polarimeters for linear incident light do not suffer from the non-uniform responses of the wave plates, even the available Glan-Thompson prisms for near-IR wavelengths do not have uniform response over thousands of nanometers.

We suggest two possible implementations of a 2-component Thomson polarimeter. With polarization-preserving fibers, existing polychromators could be modified with an additional channel to measure perpendicularly polarized light. At low T_e , the diagnostic would function as a polychromator, and at high T_e it could function as a polarimeter by summing the spectral bins for measurement of parallel polarized photons. Alternatively, the Glan-Thompson prisms could be mounted directly in the cassette to split the scattered light into parallel/perpendicular components before the fibers. This would double the number of fibers necessary, but eliminate the need for specialized polarization preserving fibers.

It is fortuitous that the 2-component polarimeter is both the most feasible option in light of the technical challenges and the best performing. Given the sub-percent error bars it is predicted to be capable of, even line radiation and APD response (quantum efficiency and additional noise enhancement factor) contributions to the errors should be well within the 10% specifications required for ITER. Since existing devices are capable of achieving sufficiently high electron temperature, experimental feasibility studies could happen in the near future.

Acknowledgments

This work supported by the U.S. Department of Energy. Thanks to the attendees of LAPD 16 for many insightful discussions.

References

- [1] I.H. Hutchinson, *Principles of Plasma Diagnostics*, Cambridge University Press, Cambridge, U.K. (2002).
- [2] J. Sheffield et al., *Plasma Scattering of Electromagnetic Radiation: Theory and Measurement Techniques*, Academic Press, Boston (2010).
- [3] T.N. Carlstrom et al., *A compact, low cost, seven channel polychromator for Thomson scattering measurements*, *Rev. Sci. Instrum.* **61** (1990) 2858.
- [4] C.L. Hsieh et al., *Silicon avalanche photodiode detector circuit for Nd:YAG laser scattering*, *Rev. Sci. Instrum.* **61** (1990) 2855.
- [5] F. Orsitto and N. Tartoni, *Proposal for a new electron temperature diagnostic for fusion reactors*, *Rev. Sci. Instrum.* **70** (1999) 798.
- [6] S.E. Segre and V. Zanza, *Polarization of radiation in incoherent Thomson scattering by high temperature plasma*, *Phys. Plasmas* **7** (2000) 2677.
- [7] V.V. Mirnov et al., *Electron kinetic effects on interferometry, polarimetry and Thomson scattering in burning plasmas*, in proceedings of IAEA Fusion Energy Conference, San Diego, U.S.A., 8–13 October 2012, [ITR/P5-32].
- [8] V.V. Mirnov et al., *Electron kinetic effects on optical diagnostics in fusion plasmas*, in proceedings of International Conference on Fusion Reactor Diagnostics, Varenna, Italy, 9–13 September 2013, in press.
- [9] G.A. Taylor et al., *The ITER Thomson scattering core LIDAR diagnostic*, 2012 JINST **7** C03043.
- [10] C. Quigg, *Relativistic Correction to Plasma Bremsstrahlung*, *Phys. Fluids* **11** (1968) 461.
- [11] O. Naito et al., *Analytic formula for fully relativistic Thomson scattering spectrum*, *Phys. Fluids* **B 5** (1993) 4256.
- [12] J.H. Williamson and M.E. Clarke, *Construction of electron distribution functions from laser scattering spectra*, *J. Plasma Phys.* **6** (1971) 211.